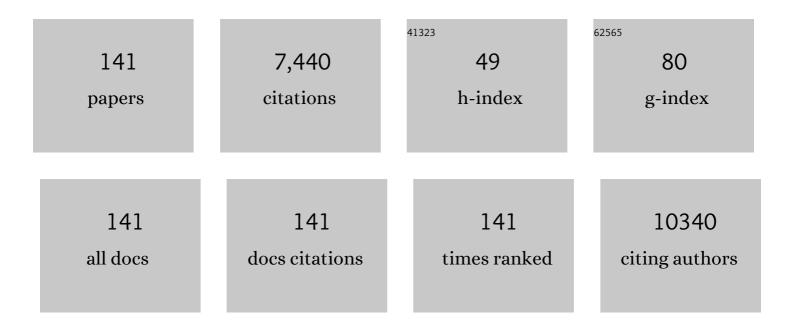
## He-You Han

List of Publications by Year in descending order

Source: https://exaly.com/author-pdf/177113/publications.pdf Version: 2024-02-01



ΗΕ-ΥΟΙΙ ΗΛΝ

#	Article	IF	CITATIONS
1	Antiviral Activity of Graphene Oxide: How Sharp Edged Structure and Charge Matter. ACS Applied Materials & Interfaces, 2015, 7, 21571-21579.	4.0	292
2	Dual-pH Sensitive Charge-Reversal Polypeptide Micelles for Tumor-Triggered Targeting Uptake and Nuclear Drug Delivery. Small, 2015, 11, 2543-2554.	5.2	234
3	Gecko-Inspired Nanotentacle Surface-Enhanced Raman Spectroscopy Substrate for Sampling and Reliable Detection of Pesticide Residues in Fruits and Vegetables. Analytical Chemistry, 2017, 89, 2424-2431.	3.2	216
4	Ratiometric Biosensor for Aggregation-Induced Emission-Guided Precise Photodynamic Therapy. ACS Nano, 2015, 9, 10268-10277.	7.3	207
5	Dualâ€Stageâ€Lightâ€Guided Tumor Inhibition by Mitochondriaâ€Targeted Photodynamic Therapy. Advanced Functional Materials, 2015, 25, 2961-2971.	7.8	205
6	Cauliflower-Inspired 3D SERS Substrate for Multiple Mycotoxins Detection. Analytical Chemistry, 2019, 91, 3885-3892.	3.2	200
7	Multi-walled carbon nanotubes can enhance root elongation of wheat (Triticum aestivum) plants. Journal of Nanoparticle Research, 2012, 14, 1.	0.8	175
8	Multisite Inhibitors for Enteric Coronavirus: Antiviral Cationic Carbon Dots Based on Curcumin. ACS Applied Nano Materials, 2018, 1, 5451-5459.	2.4	165
9	Glutathione-Capped Ag <sub>2</sub> S Nanoclusters Inhibit Coronavirus Proliferation through Blockage of Viral RNA Synthesis and Budding. ACS Applied Materials & Interfaces, 2018, 10, 4369-4378.	4.0	141
10	From Electrochemistry to Electroluminescence: Development and Application in a Ratiometric Aptasensor for Aflatoxin B1. Analytical Chemistry, 2017, 89, 7578-7585.	3.2	139
11	pHâ€Responsive, Lightâ€Triggered onâ€Demand Antibiotic Release from Functional Metal–Organic Framework for Bacterial Infection Combination Therapy. Advanced Functional Materials, 2018, 28, 1800011.	7.8	137
12	Ultrasensitive detection of aflatoxin B 1 by SERS aptasensor based on exonuclease-assisted recycling amplification. Biosensors and Bioelectronics, 2017, 97, 59-64.	5.3	128
13	Graphene Oxide-Silver Nanocomposite: Novel Agricultural Antifungal Agent against <i>Fusarium graminearum</i> for Crop Disease Prevention. ACS Applied Materials & Interfaces, 2016, 8, 24057-24070.	4.0	126
14	Acidityâ€Triggered Tumorâ€Targeted Chimeric Peptide for Enhanced Intraâ€Nuclear Photodynamic Therapy. Advanced Functional Materials, 2016, 26, 4351-4361.	7.8	122
15	A new function of graphene oxide emerges: inactivating phytopathogenic bacterium Xanthomonas oryzae pv. Oryzae. Journal of Nanoparticle Research, 2013, 15, 1.	0.8	120
16	Tumor-Triggered Geometrical Shape Switch of Chimeric Peptide for Enhanced <i>in Vivo</i> Tumor Internalization and Photodynamic Therapy. ACS Nano, 2017, 11, 3178-3188.	7.3	109
17	Carbon-Dot and Quantum-Dot-Coated Dual-Emission Core–Satellite Silica Nanoparticles for Ratiometric Intracellular Cu <sup>2+</sup> Imaging. Analytical Chemistry, 2016, 88, 7395-7403.	3.2	108
18	Endogenous stimulus-powered antibiotic release from nanoreactors for a combination therapy of bacterial infections. Nature Communications, 2019, 10, 4464.	5.8	108

#	Article	IF	CITATIONS
19	A novel method for the determination of Pb2+ based on the quenching of the fluorescence of CdTe quantum dots. Mikrochimica Acta, 2008, 161, 81-86.	2.5	107
20	Synergistic antibacterial effects of curcumin modified silver nanoparticles through ROS-mediated pathways. Materials Science and Engineering C, 2019, 99, 255-263.	3.8	107
21	Synergistic gene and drug tumor therapy using a chimeric peptide. Biomaterials, 2013, 34, 4680-4689.	5.7	105
22	A Tumor Targeted Chimeric Peptide for Synergistic Endosomal Escape and Therapy by Dualâ€&tage Light Manipulation. Advanced Functional Materials, 2015, 25, 1248-1257.	7.8	103
23	Target-triggered signal-on ratiometric electrochemiluminescence sensing of PSA based on MOF/Au/G-quadruplex. Biosensors and Bioelectronics, 2018, 118, 160-166.	5.3	103
24	Atomic Vacancies Control of Pdâ€Based Catalysts for Enhanced Electrochemical Performance. Advanced Materials, 2018, 30, 1704171.	11.1	102
25	Metal-organic frameworks-based sensitive electrochemiluminescence biosensing. Biosensors and Bioelectronics, 2020, 164, 112332.	5.3	99
26	Antiviral Activity of Graphene Oxide–Silver Nanocomposites by Preventing Viral Entry and Activation of the Antiviral Innate Immune Response. ACS Applied Bio Materials, 2018, 1, 1286-1293.	2.3	94
27	Construction of surfactant-like tetra-tail amphiphilic peptide with RGD ligand for encapsulation of porphyrin for photodynamic therapy. Biomaterials, 2011, 32, 1678-1684.	5.7	88
28	Interaction between fluorescein isothiocyanate and carbon dots: Inner filter effect and fluorescence resonance energy transfer. Spectrochimica Acta - Part A: Molecular and Biomolecular Spectroscopy, 2017, 171, 311-316.	2.0	87
29	Dual stimuli-responsive multi-drug delivery system for the individually controlled release of anti-cancer drugs. Chemical Communications, 2015, 51, 1475-1478.	2.2	85
30	Microbial synthesis of highly dispersed PdAu alloy for enhanced electrocatalysis. Science Advances, 2016, 2, e1600858.	4.7	85
31	Activable Cell-Penetrating Peptide Conjugated Prodrug for Tumor Targeted Drug Delivery. ACS Applied Materials & Interfaces, 2015, 7, 16061-16069.	4.0	84
32	Electrochemiluminecence nanogears aptasensor based on MIL-53(Fe)@CdS for multiplexed detection of kanamycin and neomycin. Biosensors and Bioelectronics, 2019, 129, 100-106.	5.3	83
33	Electrogenerated chemiluminescence from thiol-capped CdTe quantum dots and its sensing application in aqueous solution. Analytica Chimica Acta, 2007, 596, 73-78.	2.6	81
34	Application of Multiplexed Aptasensors in Food Contaminants Detection. ACS Sensors, 2020, 5, 3721-3738.	4.0	75
35	Design of Gold Hollow Nanorods with Controllable Aspect Ratio for Multimodal Imaging and Combined Chemo-Photothermal Therapy in the Second Near-Infrared Window. ACS Applied Materials & Interfaces, 2018, 10, 36703-36710.	4.0	74
36	Targeted Near-Infrared Fluorescent Turn-on Nanoprobe for Activatable Imaging and Effective Phototherapy of Cancer Cells. ACS Applied Materials & Interfaces, 2016, 8, 15013-15023.	4.0	69

#	Article	IF	CITATIONS
37	Signal-Amplified Near-Infrared Ratiometric Electrochemiluminescence Aptasensor Based on Multiple Quenching and Enhancement Effect of Graphene/Gold Nanorods/G-Quadruplex. Analytical Chemistry, 2016, 88, 8179-8187.	3.2	67
38	Engineering Nanoparticles for Optimized Photodynamic Therapy. ACS Biomaterials Science and Engineering, 2019, 5, 6342-6354.	2.6	67
39	Precisely Striking Tumors without Adjacent Normal Tissue Damage <i>via</i> Mitochondria-Templated Accumulation. ACS Nano, 2018, 12, 6252-6262.	7.3	65
40	Mitochondria-Targeted Chimeric Peptide for Trinitarian Overcoming of Drug Resistance. ACS Applied Materials & Interfaces, 2016, 8, 25060-25068.	4.0	61
41	Photothermally triggered nitric oxide nanogenerator targeting type IV pili for precise therapy of bacterial infections. Biomaterials, 2021, 268, 120588.	5.7	57
42	Miniature Hollow Gold Nanorods with Enhanced Effect for In Vivo Photoacoustic Imaging in the NIRâ€ <b>i</b> Window. Small, 2020, 16, e2002748.	5.2	56
43	Programmable DNA Tweezer-Actuated SERS Probe for the Sensitive Detection of AFB <sub>1</sub> . Analytical Chemistry, 2020, 92, 4900-4907.	3.2	56
44	Ultrasensitive SERS detection of Bacillus thuringiensis special gene based on Au@Ag NRs and magnetic beads. Biosensors and Bioelectronics, 2017, 92, 321-327.	5.3	53
45	Enzymatic biosensor of horseradish peroxidase immobilized on Au-Pt nanotube/Au-graphene for the simultaneous determination of antioxidants. Analytica Chimica Acta, 2016, 933, 89-96.	2.6	52
46	Functional peptide-based nanoparticles for photodynamic therapy. Journal of Materials Chemistry B, 2018, 6, 25-38.	2.9	52
47	A novel strategy for selective detection of Ag+ based on the red-shift of emission wavelength of quantum dots. Mikrochimica Acta, 2009, 167, 281-287.	2.5	51
48	Enzyme induced molecularly imprinted polymer on SERS substrate for ultrasensitive detection of patulin. Analytica Chimica Acta, 2020, 1101, 111-119.	2.6	51
49	Electrochemiluminescence aptasensor for multiple determination of Hg2+ and Pb2+ ions by using the MIL-53(Al)@CdTe-PEI modified electrode. Analytica Chimica Acta, 2020, 1100, 232-239.	2.6	51
50	Preparation of Mesoporous Nanosized KF/CaO–MgO Catalyst and its Application for Biodiesel Production by Transesterification. Catalysis Letters, 2009, 131, 574-578.	1.4	50
51	Clean Synthesis of an Economical 3D Nanochain Network of PdCu Alloy with Enhanced Electrocatalytic Performance towards Ethanol Oxidation. Chemistry - A European Journal, 2015, 21, 17779-17785.	1.7	50
52	Platinum Dendritic-Flowers Prepared by Tellurium Nanowires Exhibit High Electrocatalytic Activity for Glycerol Oxidation. ACS Applied Materials & Interfaces, 2015, 7, 17725-17730.	4.0	50
53	Quantum dots decorated gold nanorod as fluorescent-plasmonic dual-modal contrasts agent for cancer imaging. Biosensors and Bioelectronics, 2015, 74, 16-23.	5.3	50
54	Turn-on near-infrared electrochemiluminescence sensing of thrombin based on resonance energy transfer between CdTe/CdS core small /shell thick quantum dots and gold nanorods. Biosensors and Bioelectronics, 2016, 82, 26-31.	5.3	49

#	Article	IF	CITATIONS
55	Regulating the oxidation degree of nickel foam: a smart strategy to controllably synthesize active Ni <sub>3</sub> S <sub>2</sub> nanorod/nanowire arrays for high-performance supercapacitors. Journal of Materials Chemistry A, 2016, 4, 8029-8040.	5.2	48
56	Pt nanozyme for O <sub>2</sub> self-sufficient, tumor-specific oxidative damage and drug resistance reversal. Nanoscale Horizons, 2019, 4, 1124-1131.	4.1	48
57	Precise Chemodynamic Therapy of Cancer by Trifunctional Bacterium-Based Nanozymes. ACS Nano, 2021, 15, 19321-19333.	7.3	47
58	Structure and properties of cellulose/poly( <i>N</i> â€isopropylacrylamide) hydrogels prepared by IPN strategy. Polymers for Advanced Technologies, 2011, 22, 1329-1334.	1.6	45
59	Highly sensitive enzyme-free immunosorbent assay for porcine circovirus type 2 antibody using Au-Pt/SiO 2 nanocomposites as labels. Biosensors and Bioelectronics, 2016, 82, 177-184.	5.3	45
60	Tumor-triggered transformation of chimeric peptide for dual-stage-amplified magnetic resonance imaging and precise photodynamic therapy. Biomaterials, 2018, 182, 269-278.	5.7	45
61	Selective Thrombosis of Tumor for Enhanced Hypoxiaâ€Activated Prodrug Therapy. Advanced Materials, 2021, 33, e2104504.	11.1	45
62	Au Hollow Nanorods-Chimeric Peptide Nanocarrier for NIR-II Photothermal Therapy and Real-time Apoptosis Imaging for Tumor Theranostics. Theranostics, 2019, 9, 4971-4981.	4.6	44
63	Gastric Acid Powered Nanomotors Release Antibiotics for In Vivo Treatment of <i>Helicobacter pylori</i> Infection. Small, 2021, 17, e2006877.	5.2	44
64	In Situ Nanozymeâ€Amplified NIRâ€II Phototheranostics for Tumorâ€5pecific Imaging and Therapy. Advanced Functional Materials, 2021, 31, 2103765.	7.8	44
65	Novel Porphyrin Zr Metal–Organic Framework (PCN-224)-Based Ultrastable Electrochemiluminescence System for PEDV Sensing. Analytical Chemistry, 2021, 93, 2090-2096.	3.2	43
66	A novel method for methimazole determination using CdSe quantum dots as fluorescence probes. Mikrochimica Acta, 2009, 165, 195-201.	2.5	41
67	Ultrasmall Peptide-Coated Platinum Nanoparticles for Precise NIR-II Photothermal Therapy by Mitochondrial Targeting. ACS Applied Materials & Interfaces, 2020, 12, 39434-39443.	4.0	40
68	Excellent electrochemical performance of nitrogen-enriched hierarchical porous carbon electrodes prepared using nano-CaCO3 as template. Journal of Solid State Electrochemistry, 2013, 17, 2651-2660.	1.2	38
69	pHâ€Responsive Nanoscale Coordination Polymer for Efficient Drug Delivery and Realâ€Time Release Monitoring. Advanced Healthcare Materials, 2017, 6, 1700470.	3.9	36
70	Cancer-targeted functional gold nanoparticles for apoptosis induction and real-time imaging based on FRET. Nanoscale, 2014, 6, 9531.	2.8	35
71	Ru(bpy)32+-Silica@Poly-L-lysine-Au as labels for electrochemiluminescence lysozyme aptasensor based on 3D graphene. Biosensors and Bioelectronics, 2018, 106, 50-56.	5.3	34
72	Target triggered self-assembly of Au nanoparticles for amplified detection of Bacillus thuringiensis transgenic sequence using SERS. Biosensors and Bioelectronics, 2014, 62, 196-200.	5.3	33

#	Article	IF	CITATIONS
73	Versatile Electrochemiluminescence Assays for PEDV Antibody Based on Rolling Circle Amplification and Ru-DNA Nanotags. Analytical Chemistry, 2018, 90, 7415-7421.	3.2	32
74	Pomegranate-Inspired Silica Nanotags Enable Sensitive Dual-Modal Detection of Rabies Virus Nucleoprotein. Analytical Chemistry, 2020, 92, 8802-8809.	3.2	32
75	Dual-Mode Immunosensor for Electrochemiluminescence Resonance Energy Transfer and Electrochemical Detection of Rabies Virus Glycoprotein Based on Ru(bpy) <sub>3</sub> <sup>2+</sup> -Loaded Dendritic Mesoporous Silica Nanoparticles. Analytical Chemistry. 2022. 94. 7655-7664.	3.2	32
76	Tumor targeted gold nanoparticles for FRET-based tumor imaging and light responsive on-demand drug release. Journal of Materials Chemistry B, 2015, 3, 8065-8069.	2.9	30
77	Controlled Synthesis of Au-Island-Covered Pd Nanotubes with Abundant Heterojunction Interfaces for Enhanced Electrooxidation of Alcohol. ACS Applied Materials & amp; Interfaces, 2016, 8, 12792-12797.	4.0	30
78	Intracellular Ca2+ Cascade Guided by NIR-II Photothermal Switch for Specific Tumor Therapy. IScience, 2020, 23, 101049.	1.9	30
79	Theranostic magnetic nanoparticles for efficient capture and in situ chemotherapy of circulating tumor cells. Journal of Materials Chemistry B, 2013, 1, 3344.	2.9	29
80	Spiny-porous platinum nanotubes with enhanced electrocatalytic activity for methanol oxidation. Journal of Materials Chemistry A, 2015, 3, 1388-1391.	5.2	29
81	Fabrication of Bis-Quaternary Ammonium Salt as an Efficient Bactericidal Weapon Against <i>Escherichia coli</i> and <i>Staphylococcus aureus</i> . ACS Omega, 2018, 3, 14517-14525.	1.6	29
82	Disruption of dual homeostasis by a metal-organic framework nanoreactor for ferroptosis-based immunotherapy of tumor. Biomaterials, 2022, 284, 121502.	5.7	29
83	Recent advances in the use of near-infrared quantum dots as optical probes for bioanalytical, imaging and solar cell application. Mikrochimica Acta, 2014, 181, 1485-1495.	2.5	27
84	Acidity-Triggered Tumor Retention/Internalization of Chimeric Peptide for Enhanced Photodynamic Therapy and Real-Time Monitoring of Therapeutic Effects. ACS Applied Materials & Interfaces, 2017, 9, 16043-16053.	4.0	27
85	Activation of TRPV1 by capsaicin-loaded CaCO3 nanoparticle for tumor-specific therapy. Biomaterials, 2022, 284, 121520.	5.7	27
86	Inhibition of Porcine Epidemic Diarrhea Virus Replication and Viral 3C-Like Protease by Quercetin. International Journal of Molecular Sciences, 2020, 21, 8095.	1.8	26
87	Synthesis of p-aminothiophenol-embedded gold/silver core-shell nanostructures as novel SERS tags for biosensing applications. Mikrochimica Acta, 2011, 173, 149-156.	2.5	25
88	Probing the interactions of CdTe quantum dots with pseudorabies virus. Scientific Reports, 2015, 5, 16403.	1.6	25
89	Reasonably retard O2 consumption through a photoactivity conversion nanocomposite for oxygenated photodynamic therapy. Biomaterials, 2019, 218, 119312.	5.7	24
90	Bacteria Inspired Internal Standard SERS Substrate for Quantitative Detection. ACS Applied Bio Materials, 2021, 4, 2009-2019.	2.3	24

#	Article	IF	CITATIONS
91	Hydrogen-bonding recognition-induced aggregation of gold nanoparticles for the determination of the migration of melamine monomers using dynamic light scattering. Analytica Chimica Acta, 2014, 845, 92-97.	2.6	23
92	Enhanced immunoassay for porcine circovirus type 2 antibody using enzyme-loaded and quantum dots-embedded shell–core silica nanospheres based on enzyme-linked immunosorbent assay. Analytica Chimica Acta, 2015, 887, 192-200.	2.6	23
93	Cellular hnRNP A1 Interacts with Nucleocapsid Protein of Porcine Epidemic Diarrhea Virus and Impairs Viral Replication. Viruses, 2018, 10, 127.	1.5	23
94	Nucleobase, nucleoside, nucleotide, and oligonucleotide coordinated metal ions for sensing and biomedicine applications. Nano Research, 2022, 15, 71-84.	5.8	22
95	Bioreducible Polypeptide Containing Cell-Penetrating Sequence for Efficient Gene Delivery. Pharmaceutical Research, 2013, 30, 1968-1978.	1.7	21
96	A FRETâ€Based Dualâ€Targeting Theranostic Chimeric Peptide for Tumor Therapy and Realâ€ŧime Apoptosis Imaging. Advanced Healthcare Materials, 2014, 3, 1765-1768.	3.9	21
97	Catalytic hairpin assembly-assisted lateral flow assay for visual determination of microRNA-21 using gold nanoparticles. Mikrochimica Acta, 2019, 186, 661.	2.5	20
98	Nickel-Ion-Oriented Fabrication of Spiny PtCu Alloy Octahedral Nanoframes with Enhanced Electrocatalytic Performance. ACS Applied Energy Materials, 2019, 2, 2862-2869.	2.5	19
99	Binding induced isothermal amplification reaction to activate CRISPR/Cas12a for amplified electrochemiluminescence detection of rabies viral RNA via DNA nanotweezer structure switching. Biosensors and Bioelectronics, 2022, 204, 114078.	5.3	19
100	Cobalt ferrite nanozyme for efficient symbiotic nitrogen fixation via regulating reactive oxygen metabolism. Environmental Science: Nano, 2021, 8, 188-203.	2.2	18
101	Tea Polyphenol Liposomes Overcome Gastric Mucus to Treat Helicobacter Pylori Infection and Enhance the Intestinal Microenvironment. ACS Applied Materials & Interfaces, 2022, 14, 13001-13012.	4.0	18
102	Synthesis of multi-branched gold nanoparticles by reduction of tetrachloroauric acid with Tris base, and their application to SERS and cellular imaging. Mikrochimica Acta, 2011, 175, 55-61.	2.5	17
103	A SERS-based immunoassay for porcine circovirus type 2 using multi-branched gold nanoparticles. Mikrochimica Acta, 2013, 180, 1501-1507.	2.5	17
104	A Chimeric Peptide Logic Gate for Orthogonal Stimuli‶riggered Precise Tumor Therapy. Advanced Functional Materials, 2018, 28, 1804609.	7.8	17
105	Reduction-sensitive polypeptides incorporated with nuclear localization signal sequences for enhanced gene delivery. Journal of Materials Chemistry, 2012, 22, 13591.	6.7	16
106	The synergistic effect of a BMP-7 derived peptide and cyclic RGD in regulating differentiation behaviours of mesenchymal stem cells. Journal of Materials Chemistry B, 2014, 2, 8434-8440.	2.9	16
107	Toxicity of Molybdenum-Based Nanomaterials on the Soybean–Rhizobia Symbiotic System: Implications for Nutrition. ACS Applied Nano Materials, 2020, 3, 5773-5782.	2.4	16
108	An intelligent platform based on acidity-triggered aggregation of gold nanoparticles for precise photothermal ablation of focal bacterial infection. Chemical Engineering Journal, 2021, 407, 127076.	6.6	16

#	Article	IF	CITATIONS
109	A novel method for the analysis of calf thymus DNA based on CdTe quantum dots-Ru(bpy) 3 2+ photoinduced electron transfer system. Mikrochimica Acta, 2010, 168, 341-345.	2.5	15
110	Investigation the interaction between protamine sulfate and CdTe quantum dots with spectroscopic techniques. RSC Advances, 2016, 6, 10215-10220.	1.7	15
111	One-step synthesis of high-quality homogenous Te/Se alloy nanorods with various morphologies. CrystEngComm, 2015, 17, 3243-3250.	1.3	14
112	Robust Synthesis of Size-Dispersal Triangular Silver Nanoprisms via Chemical Reduction Route and Their Cytotoxicity. Nanomaterials, 2019, 9, 674.	1.9	14
113	DNA Nanotweezers for Biosensing Applications: Recent Advances and Future Prospects. ACS Sensors, 2022, 7, 3-20.	4.0	14
114	Interactions between Water-soluble CdSe Quantum Dots and Gold Nanoparticles Studied by UV-Visible Absorption Spectroscopy. Analytical Sciences, 2007, 23, 651-654.	0.8	12
115	A Novel Ratiometric Probe Based on Nitrogen-Doped Carbon Dots and Rhodamine B Isothiocyanate for Detection of Fe <sup>3+</sup> in Aqueous Solution. Journal of Analytical Methods in Chemistry, 2016, 2016, 1-7.	0.7	12
116	Steric shielding protected and acidity-activated pop-up of ligand for tumor enhanced photodynamic therapy. Journal of Controlled Release, 2018, 279, 198-207.	4.8	12
117	Amorphous nickel boride membrane coated PdCuCo dendrites as high-efficiency catalyst for oxygen reduction and methanol oxidation reaction. Materials Today Energy, 2019, 12, 179-185.	2.5	12
118	Development of A Super-Sensitive Diagnostic Method for African Swine Fever Using CRISPR Techniques. Virologica Sinica, 2021, 36, 220-230.	1.2	12
119	Novel gene transfer vectors based on artificial recombinant multi-functional oligopeptides. International Journal of Pharmaceutics, 2012, 436, 555-563.	2.6	11
120	Photo-Activatable Substrates for Site-Specific Differentiation of Stem Cells. ACS Applied Materials & Interfaces, 2015, 7, 23679-23684.	4.0	11
121	Self-assembly of Pt-based truncated octahedral crystals into metal-frameworks towards enhanced electrocatalytic activity. Journal of Materials Chemistry A, 2016, 4, 15169-15180.	5.2	11
122	Preparation of Modified Konjac Glucomannan Nanoparticles and their Application as Vaccine Adjuvants to Promote Ovalbumin-Induced Immune Response in Mice. Pharmaceutical Research, 2018, 35, 105.	1.7	11
123	Early diagnosis of rabies virus infection by RPA-CRISPR techniques in a rat model. Archives of Virology, 2021, 166, 1083-1092.	0.9	10
124	Near-infrared electrogenerated chemiluminescence from quantum dots. Reviews in Analytical Chemistry, 2013, 32, .	1.5	9
125	Synthesis of Tellurium Fusiform Nanoarchitectures by Controlled Living Nanowire Modification. Journal of Physical Chemistry C, 2016, 120, 12305-12312.	1.5	9
126	Pd@Pt Core–Shell Nanodots Arrays for Efficient Electrocatalytic Oxygen Reduction. ACS Applied Nano Materials, 2019, 2, 3695-3700.	2.4	9

#	Article	IF	CITATIONS
127	An aqueous platinum nanotube based fluorescent immuno-assay for porcine reproductive and respiratory syndrome virus detection. Talanta, 2015, 144, 324-328.	2.9	7
128	Sensitive immunoassay for porcine pseudorabies antibody based on fluorescence signal amplification induced by cation exchange in CdSe nanocrystals. Mikrochimica Acta, 2013, 180, 303-310.	2.5	6
129	Intravital imaging of Bacillus thuringiensis Cry1A toxin binding sites in the midgut of silkworm. Analytical Biochemistry, 2014, 447, 90-97.	1.1	6
130	Evaluation of Biological Toxicity of CdTe Quantum Dots with Different Coating Reagents according to Protein Expression of Engineering <i>Escherichia coli</i> . Journal of Nanomaterials, 2015, 2015, 1-7.	1.5	6
131	A New Type of Capping Agent in Nanoscience: Metal Cations. Small, 2019, 15, 1900444.	5.2	6
132	Biogenic Hybrid Nanosheets Activated Photothermal Therapy and Promoted Anti-PD-L1 Efficacy for Synergetic Antitumor Strategy. ACS Applied Materials & Interfaces, 2020, 12, 29122-29132.	4.0	6
133	Sequential assembled chimeric peptide for precise synergistic phototherapy and photoacoustic imaging of tumor apoptosis. Chemical Engineering Journal, 2022, 427, 130775.	6.6	6
134	A spatial and cellular distribution of rabies virus infection in the mouse brain revealed by fMOST and singleâ€cell RNA sequencing. Clinical and Translational Medicine, 2022, 12, e700.	1.7	6
135	Pd–Au heterostructured nanonecklaces with adjustable interval and size as a superior catalyst for degradation of 4-nitrophenol. CrystEngComm, 2017, 19, 5686-5691.	1.3	5
136	Multifunctional Nanosystems with Enhanced Cellular Uptake for Tumor Therapy. Advanced Healthcare Materials, 2022, 11, e2101703.	3.9	5
137	Novel approach to enhance Bradyrhizobium diazoefficiens nodulation through continuous induction of ROS by manganese ferrite nanomaterials in soybean. Journal of Nanobiotechnology, 2022, 20, 168.	4.2	5
138	Two-dimensional colloidal crystal assisted formation of conductive porous gold films with flexible structural controllability. Journal of Colloid and Interface Science, 2015, 437, 291-296.	5.0	4
139	Timeâ€resolved fluorescent microsphere lateral flow biosensors for rapid detection of <i>Candidatus</i> Liberibacter asiaticus. Plant Biotechnology Journal, 2022, 20, 1235-1237.	4.1	4
140	Cancer Treatment: Dual-Stage-Light-Guided Tumor Inhibition by Mitochondria-Targeted Photodynamic Therapy (Adv. Funct. Mater. 20/2015). Advanced Functional Materials, 2015, 25, 2942-2942.	7.8	0
141	Light-Induced Caspase-3-Responsive Chimeric Peptide for Effective PDT/Chemo Combination Therapy with Good Compatibility. ACS Applied Bio Materials, 2020, 3, 2392-2400.	2.3	0